



# Deep Learning-Based Image Reconstruction in Musculoskeletal MRI

## 근골격 자기공명영상에서의 딥러닝 기반 영상 재구성 기법

Hye Jin Yoo, MD\*

Department of Radiology, Seoul National University Hospital, Seoul, Korea

MRI plays a vital role in obtaining high-quality images for evaluating the complex anatomical structures of the musculoskeletal system. However, its long acquisition time can lead to patient discomfort and motion artifacts, which degrade image quality. To overcome this limitation, parallel imaging techniques such as Sensitivity Encoding (SENSE) and Generalized Autocalibrating Partial Parallel Acquisition (GRAPPA) were developed, followed by compressed sensing, which reconstructs images from undersampled k-space data using iterative methods. More recently, deep learning-based image reconstruction techniques have emerged, offering improved signal-to-noise ratio and higher acceleration factors. Recent studies evaluating various joints—including the spine, knee, ankle, and shoulder—have shown that deep learning-based reconstruction significantly reduces scan times while maintaining image quality and diagnostic performance comparable to conventional methods, supporting broader clinical application. Additionally, ongoing research aims to enhance image resolution in low-field MRI systems and correct various artifacts, further expanding the potential of these advanced techniques.

**Index terms** Deep Learning; Magnetic Resonance Imaging; Image Post Processing;  
Parallel Imaging; Musculoskeletal Disease

## INTRODUCTION

A major advantage of MRI is its ability to provide high-resolution anatomical and functional images without the use of ionizing radiation. MRI is particularly sensitive to physical properties such as T1 and T2 relaxation times, diffusion, and blood flow, allowing it to depict distinct anatomical and physiological characteristics (1). However, a significant drawback of MRI is its prolonged acquisition time, which increases patient discomfort and the likelihood of motion, resulting in artifacts that degrade image quality.

Received February 19, 2025

Revised April 9, 2025

Accepted June 27, 2025

\*Corresponding author

Hye Jin Yoo, MD

Department of Radiology,  
Seoul National University Hospital,  
101 Daehak-ro, Jongno-gu,  
Seoul 03080, Korea.

Tel 82-2-2072-0856

Fax 82-2-743-6385

E-mail dalnara3@snu.ac.kr

This is an Open Access article distributed under the terms of the Creative Commons Attribution Non-Commercial License (<https://creativecommons.org/licenses/by-nc/4.0/>) which permits unrestricted non-commercial use, distribution, and reproduction in any medium, provided the original work is properly cited.

To address this issue, parallel imaging (PI) techniques were developed, with Sensitivity Encoding (SENSE; Philips Healthcare; Best, Netherlands) and GeneRalized Autocalibrating Partial Parallel Acquisition (GRAPPA; Siemens Healthineers, Erlangen, Germany) being among the most widely used methods (2). These techniques reconstruct images from undersampled k-space data by utilizing coil sensitivity maps or by supplementing missing data using information from surrounding coils. Subsequently, compressed sensing (CS) was introduced as another acceleration technique. CS reconstructs images from randomly undersampled k-space data through iterative methods, enabling scan time reduction while preserving image quality comparable to that of fully sampled data (2).

With the rapid advancement of AI, deep learning (DL) has been incorporated into accelerated MR imaging. In 2016, the first method for accelerated MR image acquisition using deep learning-based reconstruction (DLR) was introduced, and this approach has continued to evolve (3). Compared to conventional acceleration techniques, DLR provides a higher signal-to-noise ratio (SNR) and allows for higher acceleration factors (AFs) (4).

Musculoskeletal imaging, in particular, requires high-resolution imaging due to the complexity and variability of anatomical structures. Achieving such resolution often necessitates longer scan times, which increase patient discomfort and the risk of motion-related artifacts. Moreover, musculoskeletal MRI is often performed on patients experiencing pain or functional impairment, making it particularly challenging to obtain high-quality images quickly. As such, musculoskeletal imaging is a field where accelerated MR imaging techniques capable of producing high-quality images in a shorter time are especially crucial.

## CONVENTIONAL ACCELERATED MRI TECHNIQUES

### PARALLEL IMAGING (PI)

The total acquisition time (TA) in MRI can be expressed by the following equation:

$$TA = \text{number of acquired phase encodings (}N_y\text{)} \times \text{repetition time (TR)} \times \text{number of signal averages (}N_A\text{)}$$

To reduce the TA, either the TR must be shortened or the number of data points acquired along the phase-encoding direction must be reduced. Shortening the TR requires rapid gradient switching, which may lead to peripheral nerve stimulation or excessive energy deposition in the patient, raising safety concerns. Reducing the number of phase-encoding lines—i.e., undersampling—decreases the field of view, which can result in aliasing artifacts (Fig. 1). The purpose of PI is to eliminate these artifacts and reconstruct the original image.

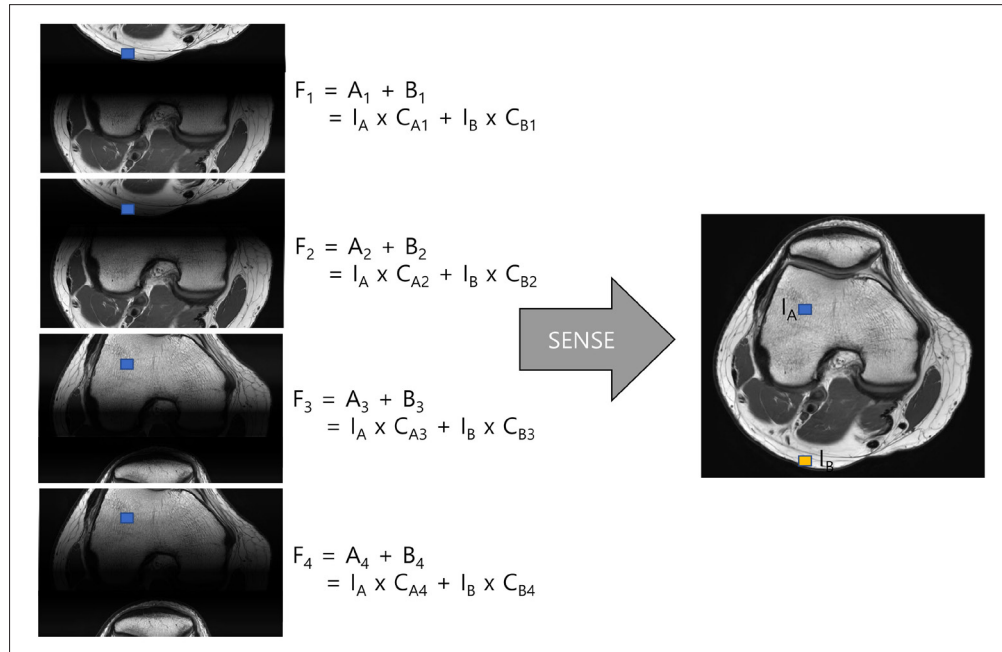
In Cartesian sampling, PI methods are classified into two categories: image-domain and k-space domain techniques. SENSE represents the image-domain approach, while GRAPPA represents the k-space domain approach (1, 5, 6).

### SENSITIVITY ENCODING (SENSE)

SENSE reduces acquisition time through undersampling, and the reduction factor (R) indicates the degree of scan time reduction (e.g., R = 2 halves the scan time). Undersampling introduces aliasing artifacts, which are resolved using multiple receiver coils with different sensitivity maps. One limitation of this method is that the SNR decreases as fewer data are

**Fig. 1.** SENSE reconstruction for a uniform Cartesian acceleration of  $R = 2$  with four coils shows signals from two equally spaced pixels aliased onto the same pixel in the reduced field of view image, and the system solves for the original values using known coil sensitivities and pixel intensities.

SENSE = Sensitivity Encoding



acquired. SNR loss can be described by the geometry factor (G-factor), as shown in the equation (Fig. 1):

$$\text{SNR}_{\text{accelerated}}(x, y) = \text{SNR}_{\text{full}}(x, y)/g(x, y)\sqrt{R}$$

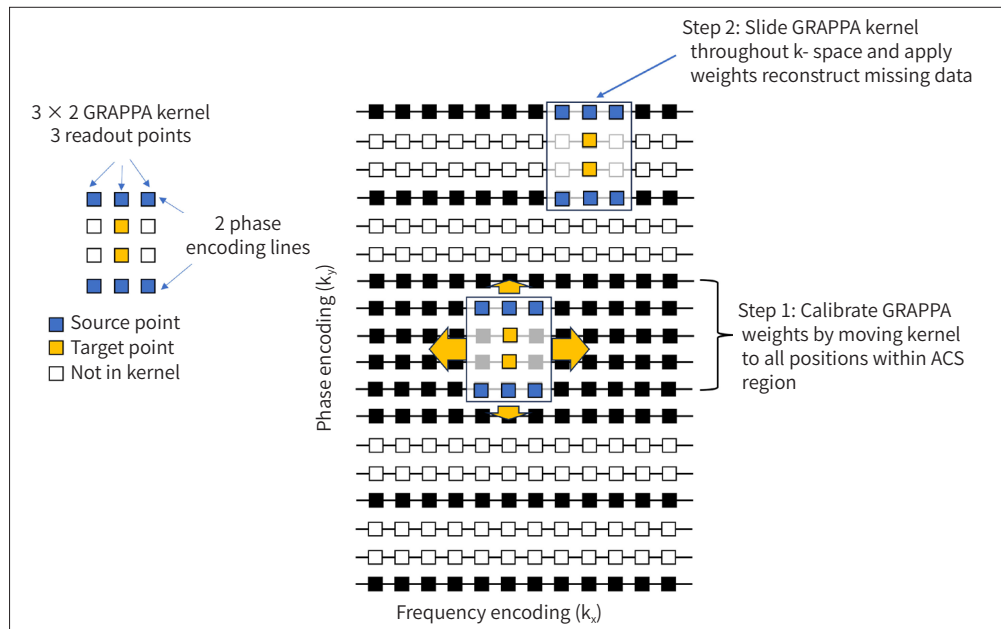
Another limitation is the potential for image distortion due to inaccuracies in coil sensitivity maps.

#### GENERALIZED AUTOCALIBRATING PARTIAL PARALLEL ACQUISITION (GRAPPA)

GRAPPA fills in missing k-space data (target points) by linearly combining nearby acquired points (source points) (Fig. 2). Specifically, GRAPPA estimates target points by applying weights to adjacent source points and summing the results. These weights are derived from calibration data, known as the auto-calibration signal (ACS), which are acquired from the center of k-space where both source and target data are available. A reconstruction kernel is moved across this region, and the weights that best predict the target points from the source points are computed. These weights are then applied to the skipped phase-encoding lines during accelerated imaging to reconstruct the missing data (1, 7).

Because GRAPPA does not depend on coil sensitivity maps, it can be used reliably even in situations where sensitivity maps are difficult to obtain, such as in areas with low signal intensity or when significant patient motion is present.

**Fig. 2.** GRAPPA reconstruction illustrates a  $3 \times 2$  kernel applied for  $R = 3$  acceleration and demonstrates how calibration lines are used to calculate GRAPPA weights for reconstructing missing k-space data.  
ACS = auto-calibration signal, GRAPPA = GeneRalized Autocalibrating Partial Parallel Acquisition



## SIMULTANEOUS MULTI-SLICE IMAGING (SMS)

Simultaneous Multi-Slice Imaging (SMS) is an acceleration technique that uses multiband RF pulses to excite multiple slices simultaneously. While the PI methods discussed above reconstruct images within a single slice using coil sensitivity differences, SMS acquires multiple slices at once and then separates the overlapped slices based on coil sensitivity variations. The core principle is the ability to acquire several slices in the time typically required to acquire one, thereby reducing TA. The number of slices acquired simultaneously is referred to as the multiband factor.

SMS offers several advantages: it reduces total scan time, increases the SNR compared to SENSE and GRAPPA, and is less sensitive to motion. However, a limitation of SMS is the increased specific absorption rate (SAR) due to the higher number of radiofrequency (RF) pulses. This is particularly concerning in patients with metallic implants, where localized SAR elevation can cause tissue damage.

To mitigate such risks, techniques such as reducing RF peak power using the variable-rate selective excitation (VERSE) algorithm, applying periodically spaced RF pulses (PINS pulses), or using specialized transmit coil geometries (parallel RF transmission) have been developed to lower SAR and improve patient safety (6).

## CONTROLLED ALIASING IN PARALLEL IMAGING RESULTS IN HIGHER ACCELERATION (CAIPIRINHA)

In three-dimensional (3D) imaging, adding the slice-encoding direction to the conventional phase-encoding direction results in longer acquisition times (1). However, acceleration can be applied in both the phase-encoding and slice-encoding directions, and the overall AF is the

product of the AFs applied in each direction.

In conventional 2D imaging, due to geometric and sensitivity differences among coils, there is a tendency for amplified noise and residual aliasing, which limits the achievable AF to around 3 or 4 (1, 6). In contrast, 3D imaging allows for the application of moderate AFs in both encoding directions while maintaining image quality, thereby enabling significantly higher total acceleration through the multiplication of the two AFs.

Furthermore, because the entire excited volume contributes signal in 3D imaging, the SNR is typically higher than in 2D PI. In Controlled Aliasing in Parallel Imaging Results in Higher Acceleration (CAIPIRINHA), acceleration is applied simultaneously in both encoding directions. As shown in Fig. 3, k-space is sampled in a zigzag pattern, which helps reduce aliasing artifacts.

## COMPRESSED SENSING (CS)

CS in MRI is analogous to compression techniques used in digital images, such as JPEG. The principle is based on the observation that many pixels in an image carry redundant or similar information, so a complete image can be accurately reconstructed even when only a subset of the data is known. Three key components are required to achieve this (1, 8, 9):

## INCOHERENT UNDERSAMPLING

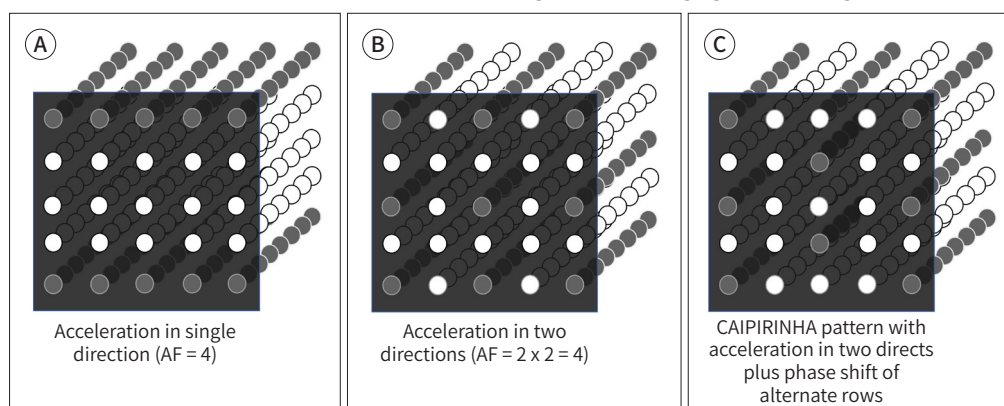
To reduce acquisition time, data are undersampled in a pseudo-random manner. Regular undersampling typically results in aliasing artifacts. However, when undersampling is performed randomly, the artifacts appear as incoherent noise across the image, making them easier to suppress during post-processing. Since the central region of k-space contains most of the critical image information, CS generally oversamples this region. Thus, the sampling pattern is not completely random but partially randomized.

## SPARSIFYING TRANSFORMATION

Not all pixels in an image carry meaningful information. Therefore, when storing the im-

**Fig. 3.** CAIPIRINHA reconstruction demonstrates how modified sampling patterns and phase shifts distribute aliasing artifacts across slices, enabling higher AFs with improved image quality: (A) acceleration in one direction (AF = 4), (B) acceleration in two directions (AF = 2 × 2 = 4), and (C) CAIPIRINHA with added phase shifts in alternate rows.

AF = acceleration factor, CAIPIRINHA = Controlled Aliasing in Parallel Imaging Results in Higher Acceleration



age, only the significant pixels are retained, while the less informative ones can be discarded without significantly compromising the reconstruction. For example, in MR angiography, the background is mostly dark with little useful information, while the vessels appear bright. Retaining only the vessel information allows for accurate image reconstruction. Such images are considered sparse. However, in cases like brain MRI, where most pixels contain relevant information, the image is not naturally sparse. In these situations, mathematical transformations—such as wavelet transforms—are used to convert the image into a sparse domain. This is referred to as a sparsifying transformation.

### ITERATIVE RECONSTRUCTION

There is a trade-off between maintaining data consistency (preserving information from the original image) and enforcing sparsity (suppressing noise). Giving too much weight to data consistency can amplify noise, while overemphasizing sparsity can cause significant loss of detail. Iterative reconstruction solves this by gradually balancing these competing goals to find an optimal solution—an image that preserves the maximum amount of useful information with minimal noise. This refinement process continues until a satisfactory result is achieved.

Table 1 summarizes the terminology used for each of these techniques.

### DEEP LEARNING-BASED ACCELERATED MRI TECHNIQUES

DLR is a technique that applies DL algorithms to undersampled k-space data to reconstruct MR images, thereby improving image quality, increasing acquisition speed, and enhancing diagnostic accuracy (Figs. 4, 5) (5, 6, 10-12).

As described earlier, both PI and CS accelerate image acquisition by undersampling k-space data; however, they are inherently limited by low SNR and aliasing artifacts. Although CS provides higher SNR than PI, it is often associated with image blurring. DLR has emerged as a promising technique that addresses these limitations. It reconstructs high-quality images from rapidly acquired data using DL models. Numerous studies have evaluated whether DLR can maintain diagnostic performance, reduce artifacts, and shorten scan time (5, 13).

In 2016, Wang et al. (3) first demonstrated the feasibility of reconstructing accelerated MR images using DL models. Since then, DL has been actively investigated for other related ap-

**Table 1.** Vendor MRI Acronyms

	Siemens Healthineers	GE Healthcare	Philips Healthcare	Canon Medical Systems
Image domain PI	mSENSE	ASSET	SENSE	SPEEDER
k-space domain PI	GRAPPA	ARC		
CS	Compressed Sensing	HyperSense	Compressed SENSE	Compressed SPEEDER (CS with PI)
SMS	Simultaneous Multi-Slice	HyperBand	MultiBand SENSE	MultiBand SPEEDER
DL reconstruction	Deep Resolve Gain/Boost/Sharp	AIR™ Recon DL Sonic DL		AiCE

AiCE = Advanced intelligent Clear IQ Engine, ARC = Autocalibrating Reconstruction for Cartesian imaging, ASSET = array spatial sensitivity encoding technique, CS = compressed sensing, DL = deep learning, GRAPPA = GeneRalized Autocalibrating Partial Parallel Acquisition, PI = parallel imaging, SENSE = Sensitivity Encoding, SMS = simultaneous multislice imaging

**Fig. 4.** Comparison of conventional and (A) DL-based reconstruction (B “AIR Recon DL”, GE Healthcare) of accelerated ankle MRI in a 27-year-old female shows that the DL-reconstructed image at acceleration factor = 3 maintains comparable quality to the non-accelerated image, (C) although trabecular textures appear slightly blurred and overly smoothed.

DL = deep learning



**Fig. 5.** Comparison of conventional and (A) DL-based reconstruction (B “SwiftMR”, AIRS Medical) of accelerated spine MRI in a 29-year-old male shows that the DL-reconstructed image at acceleration factor = 2 reduces noise and improves quality compared to the non-accelerated image (C), despite a significant scan time reduction, though with slightly blurred textures.

DL = deep learning



plications, such as super-resolution (converting low-resolution images into high-resolution ones), artifact reduction, and motion correction (5).

## RECONSTRUCTION OF UNDERSAMPLED K-SPACE DATA

Most DLR techniques are developed by training neural networks to minimize the difference between undersampled and fully sampled data through iterative learning (6, 10, 14-16). Table 1 summarizes the commercial product names of currently available DLR technologies.

## DATA-DRIVEN END-TO-END METHOD

This approach employs neural networks such as U-Net, Residual Network (ResNet), and

Generative Adversarial Network (GAN), which were originally developed for use in other fields. The network is trained to map input data (undersampled k-space data or aliased images) to the corresponding output data (fully sampled k-space data or high-quality images) (Fig. 6) (6, 10, 14-16). The architecture between the input and output functions as a complete “black box,” and a large amount of training data is required to train such models effectively (17).

Data-driven end-to-end reconstruction methods can be categorized into three types based on the domain in which training occurs: image domain, k-space learning, and direct mapping (Fig. 7) (10, 13, 14).

**Fig. 6.** The deep learning MR reconstruction framework begins with undersampled input and integrates prior knowledge such as coil sensitivity, enabling the trained network to reconstruct high-quality images through learned backpropagation.

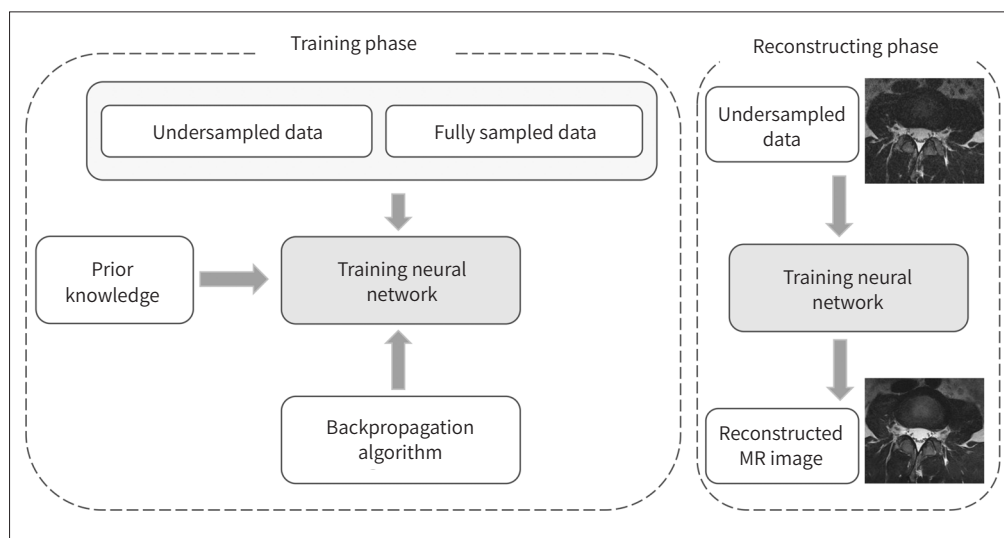
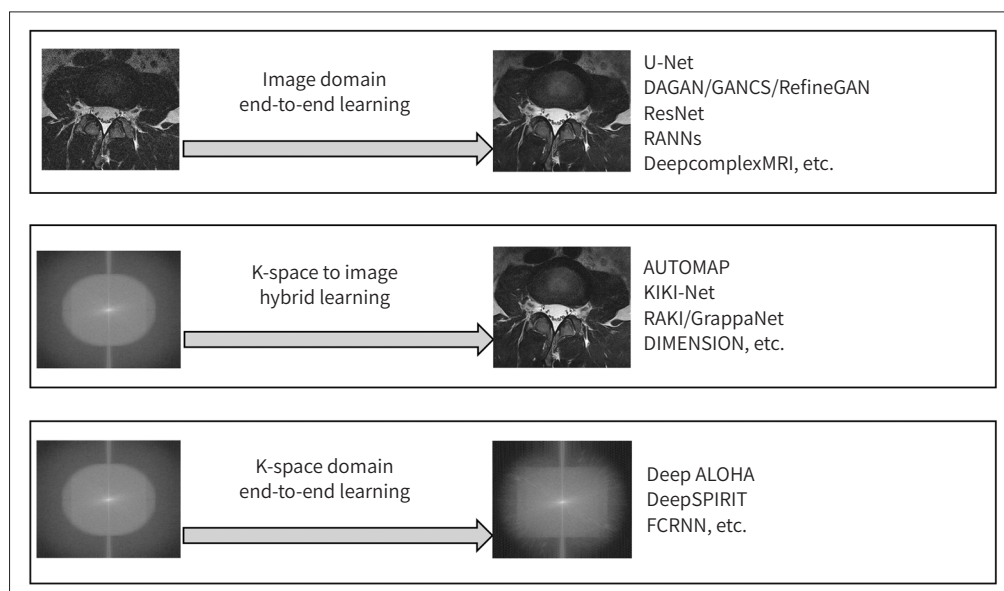


**Fig. 7.** End-to-end deep learning MR image reconstruction is illustrated with three subtypes: image domain models refine initial images, hybrid models combine k-space and image domain features, and k-space domain models reconstruct missing data directly before image transformation.



The image domain type trains a deep neural network to refine an initial image reconstructed from undersampled k-space data, making it resemble the fully sampled reference image. This approach is particularly effective in reducing noise and eliminating artifacts.

The k-space learning type focuses on enhancing the quality of k-space data itself. Training is performed using information from the MR system, such as phase and coil sensitivity data. The initial k-space data are input into the neural network, which outputs refined k-space data. The final MR image is then reconstructed from this enhanced k-space. This method is especially effective in preserving low-frequency k-space components, allowing for better retention of image detail and fine anatomical structures.

The direct mapping type takes k-space data as input and directly generates MR images as output. This method has the advantage of minimizing errors caused by magnetic field inhomogeneities, eddy currents, and phase distortions (10).

### MODEL-DRIVEN UNROLLED OPTIMIZATION

This approach represents another DLR method, integrating CS with DL principles (17). The process begins by constructing a mathematical model grounded in prior knowledge—specifically, the optimization problems defined in CS. An iterative reconstruction algorithm is then developed to solve this problem. Finally, the iterations of the algorithm are unrolled into a DL network, with each iteration represented as a single network layer (17).

In this framework, a deep network composed of multiple layers—each with distinct weights and activation functions—progressively transforms the input data to extract higher-level features. Examples include variational networks and deep cascade networks.

Variational networks are based on traditional CS models and operate by unrolling the iterations of a gradient descent algorithm within the network while learning relevant parameters. Compared to purely data-driven methods, this approach offers greater interpretability during the iterative process, requires less training data, and involves fewer manually tuned parameters (6).

Additionally, because this method emphasizes data consistency, it is more effective in suppressing hallucination artifacts or nonexistent features in the reconstructed images, thereby enabling more reliable and consistent image reconstruction.

### SUPER-RESOLUTION IMAGING

Super-resolution imaging refers to the reconstruction of high-resolution images from low-resolution inputs. Traditional methods for improving spatial resolution, such as zero filling, bicubic interpolation, and B-spline interpolation, increase matrix size and enhance image quality. However, with the advancement of DL, super-resolution techniques have increasingly been applied in this field. DL algorithms have been developed to convert low-resolution MR images into high-resolution counterparts (Figs. 8, 9, Table 2) (6, 18, 19).

Chaudhari et al. (20) developed a 3D Convolutional Neural Network (CNN) algorithm that transforms low-resolution double-echo steady-state (DESS) images into high-resolution images. Their study demonstrated improvements not only in cartilage image quality but also in osteophyte detection and cartilage segmentation.

In another study, a U-Net-based method was used to enhance the resolution of 3D DESS

**Fig. 8.** Super-resolution reconstruction of cervical spine MRI “Deep Resolve Boost/Sharp” (Siemens Korea Research MRI Center), (A) shows that the deep learning-based image increases resolution (matrix 640 × 640) and sharpness compared to the conventional low-resolution image (matrix 320 × 320) (B).

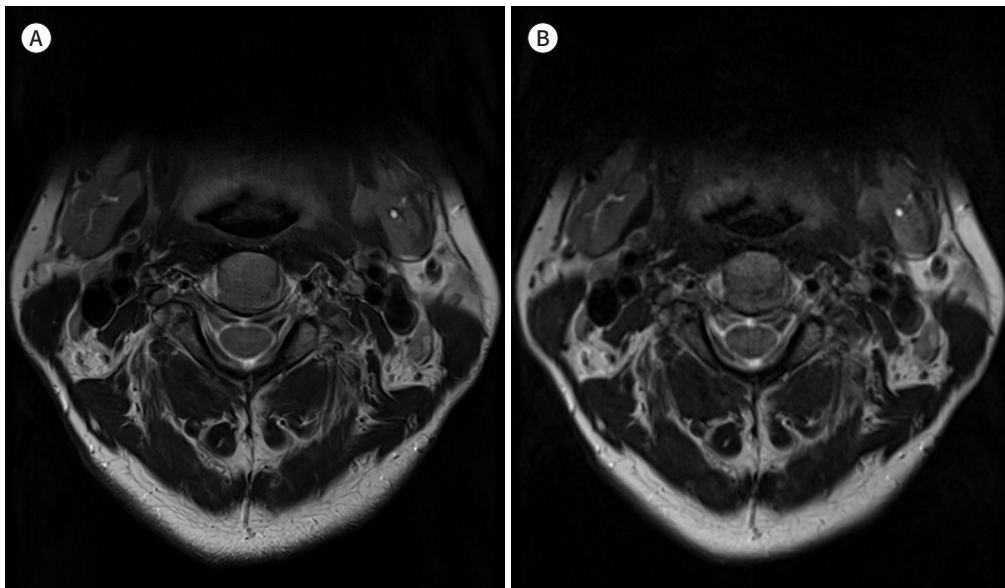
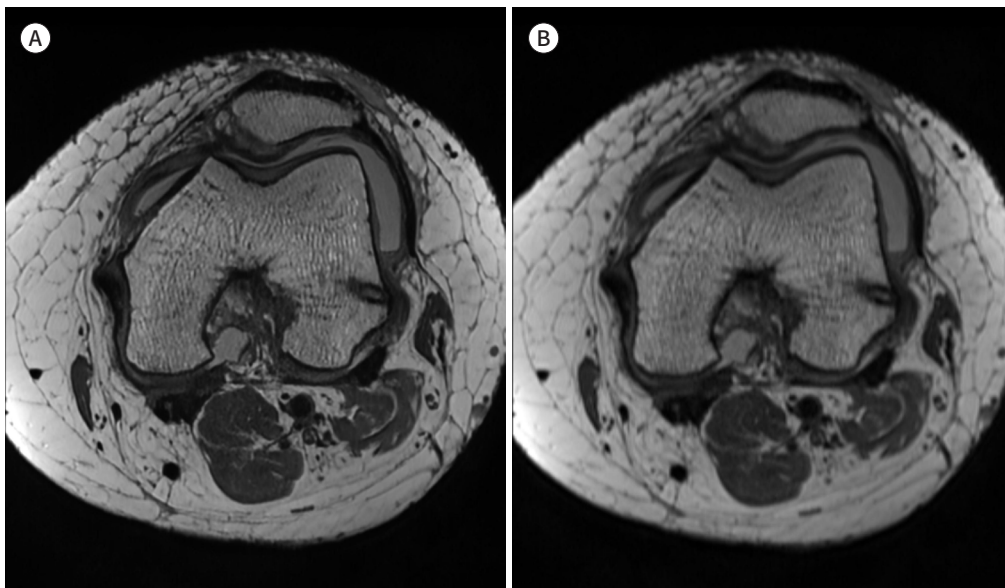


**Fig. 9.** Super-resolution reconstruction of knee MRI (“SwiftMR”, AIRS Medical) (A) shows that the deep learning-based image improves resolution and sharpness compared to the conventional low-resolution image (B).



images, which improved delineation between cartilage and surrounding soft tissues (21).

Qiu et al. (22) proposed an Efficient Medical Image Super-Resolution (EMISR) algorithm that combines the strengths of conventional super-resolution CNNs and the efficient sub-pixel CNN (ESPCN) approach. This method improved edge detail while reducing image reconstruction time. Furthermore, another study confirmed that converting to high-resolution images could be achieved without compromising the integrity of quantitative T2 relaxation time maps in cartilage (23).

**Table 2.** Key Differences of DLR and SR

Feature	DLR	SR
Primary goal	Correct artifacts, noise, and limitations of data acquisition	Increase image resolution beyond what was acquired
Input	Raw k-space data (incomplete or noisy)	Reconstructed, low-resolution MR images
Output	Reconstructed image (potentially same resolution as standard protocol)	High-resolution image
Focus	Data acquisition process	Image post-processing
Problem solved	Artifacts, noise, undersampling	Resolution limitations

DLR = deep learning-based reconstruction, SR = super-resolution

## ARTIFACT CORRECTION

Musculoskeletal MRI is particularly sensitive to motion due to its inherently long acquisition times. Patient motion can result in various artifacts, such as blurring, ringing, and ghosting, which not only degrade image quality but also hinder the detailed evaluation of intra-articular structures. DLR techniques have been explored as promising tools for correcting motion-related artifacts caused by involuntary patient movement and physiological processes such as respiration (24, 25).

Several studies have trained deep neural networks using simulated or volunteer data to identify and correct motion artifacts. These methods have been successfully applied to various anatomical regions, including the brain, abdomen, and pelvis, improving image quality without compromising morphological detail. Küstner et al. (25) employed autoencoder- and GAN-based architectures for retrospective motion correction and demonstrated sufficient image quality in pelvic MRI using both approaches. Motion artifacts from random hip movements and periodic motion were effectively suppressed, with the GAN-based MedGAN model producing nearly artifact-free images that closely resembled motion-free acquisitions.

Desai et al. (26) proposed a semi-supervised consistency training framework called VORTEX. This model incorporates both image-based augmentation (e.g., flipping, scaling, rotation, translation, shearing) and physics-based augmentation (e.g., noise, motion). Singh et al. (27) developed a data-consistency-based motion artifact mitigation method by simulating motion during training and estimating motion during inference.

Despite these advancements, clinical implementation of motion-correction techniques in musculoskeletal MRI remains limited.

## CLINICAL APPLICATIONS OF DEEP LEARNING-BASED RECONSTRUCTION (DLR)

Major studies applying DLR techniques in musculoskeletal MRI are summarized in Table 3.

### SPINE MRI

Fervers et al. (28) compared AI-based CS (CS-AI) with conventional CS in 3D T2-weighted spine imaging and demonstrated that CS-AI provided significantly higher SNR for bone structures ( $p = 0.0129$ ). Qualitative assessments of other spinal structures also favored CS-AI ( $p < 0.001$ ). Notably, with AFs of 8 or 11, image quality with conventional CS deteriorated to

**Table 3.** Clinical Studies of Deep-Learning Based MR Image Reconstruction in Musculoskeletal Systems

First author and year	MRI Scanner and Vendor	Acceleration Factors	Techniques and Factors	Sequence	Time Reduction	Summary
<b>Spine</b>						
Fervers (2023)	3-T Ingenia (Philips Healthcare)	SENSE vs. CS (4, 5, 8, 11) vs. CS-AI (4, 5, 8, 11)	3D TSE T2WI	CS4.5 (38.88%), CS 8 (65.11%), CS 11 (74.47%)	The CS-AI 4.5 sequence was subjectively rated better than the standard technique. In the objective rating, only a SNR of the bone showed a significant tendency towards better results of the deep-learning-based reconstructions. CS in combination with deep-learning-based image reconstruction allows for stronger undersampling of k-space data without loss of image quality, and thus has potential for further scan time reduction	
Sui (2023)	3-T uMR780 (United Imaging Healthcare)	Standard vs. CS-AI	2D T2WI, T1WI, FS T2WI	18.87%	CS-AI acquisition method enabled an approximately 18.87% reduction in examination time ( $p < 0.001$ ) and that CS-AI was interchangeable with standard 2D sequences. CS-AI showed reduced artifacts compared to 2D sequences	
Almansour (2023)	1.5-T and 3-T MAGNETOM scanners (Siemens Healthineers)	Standard vs. CS-AI	2D TSE T2WI, T1WI	70%	CS-AI method was found to be interchangeable with standard 2D sequences for detecting various abnormalities of the spine at MRI. CS-AI acquisition provided excellent image quality, with a 70% reduction in examination time	
Schllicht (2024)	0.55-T Siemens MAGNETOM scanners (Siemens Healthineers)	Conventional vs. advanced DL-based post-processing techniques	2D TSE T2WI, T1WI, TIRM	44.40%	DLR improve the visually perceived image quality in lumbar spine imaging at 0.55 T while simultaneously allowing to substantially decrease image acquisition times (44.4%)	
<b>Knee</b>						
Herrmann (2021)	3-T MAGNETOM PrismaFit (Siemens Healthcare)	Conventional TSE (TSE <sub>s</sub> ) vs. DL-based TSE (TSE <sub>DL</sub> )	2D TSE PDWI + FS	51%	Overall image quality was rated to be excellent, with a significant improvement in edge sharpness and reduced noise compared to TSE <sub>s</sub> ( $p < 0.001$ ). No difference was found concerning the extent of artifacts, the delineation of anatomical structures, and the diagnostic confidence comparing TSE <sub>s</sub> and TSE <sub>DL</sub> ( $p > 0.05$ ). Therefore, DL image reconstruction for TSE sequences in MSK imaging is feasible, enabling a remarkable time saving (up to 75%), whilst maintaining excellent image quality and diagnostic confidence	
Johnson (2023)	3-T MAGNETOM Skyra and Biograph mMR (Siemens Healthineers)	Conventional (PI) vs. DL-based image (AI-PI)	2D TSE T2WI, PDWI	44%	The DL-reconstructed images enabled a nearly twofold reduction in scan time for a knee MRI and were determined to be of diagnostic equivalence with the conventional images for detection of abnormalities. The overall image quality score was significantly better ( $p < 0.001$ ) for the DL than for the conventional images	
Iuga (2023)	3-T Ingenia (Philips Healthcare)	CS vs. CS-AI (1, 2, 3, 4, and 6)	2D TSE PDWI + FS	CS-AI 2 (47.48%), CS-AI 3 (64.04%), CS-AI 4 (71.92%), CS-AI 6 (80.13%)	CS-AI images maintained similar image quality to the reference, which would allow for a reduction in scan time of 64% with unchanged image quality compared to the unaccelerated sequence. SNR and CNR were significantly higher for all CS-AI reconstructions compared to CS (all $p < 0.05$ )	

**Table 3.** Clinical Studies of Deep-Learning Based MR Image Reconstruction in Musculoskeletal Systems (Continued)

First author and year	MRI Scanner and Vendor	Acceleration Factors	Techniques and Sequence	Time Reduction	Summary
Wang (2023)	3-T uMR780 (United Imaging Healthcare)	PI vs CS-AI (3.5 min) vs. CS-AI (2 min)	2D TSE PDWI+FS, T1WI	CS-AI (3.5 min) (56.25%) vs. CS-AI (2 min) (75%)	Compared with the conventional PI acquisition, the novel CS-AI protocol demonstrated superior image quality and was feasible for achieving equivalent detection of structural abnormalities (meniscal tears, cruciate ligament tears, and cartilage defects) while reducing acquisition time by half
Dratsch (2024)	3-T Ingenia (Philips Healthcare)	SENSE (2) vs. CS (10,13,15,17) vs. CS-AI (10,13,15,17)	3D PDWI-FS	54%-73%	The 3D images reconstructed with CS-AI showed that tenfold acceleration may be feasible without significant loss of quality when compared to the conventional compressed sensing ( $p \geq 0.999$ ). 54% faster image acquisition may be possible
Ni (2024)	3-T uMR780 (United Imaging Healthcare)	2D PI vs. 3D CS vs. 3D CS-AI (5.72-16.34)	2D T1WI, PDWI-FS, 3D MPR (2 mm or 3.5 mm)	3D CS-AI (10.69) (58%)	An acceleration factor of 10.69 × was identified as optimal. The quality evaluation showed that 3D-ACS provided poorer bone structure visualization, and improved cartilage visualization and less satisfactory axial images with 3.5 mm/2.0 mm MPR than PI. High levels of diagnostic agreement ( $k: 0.81-0.94$ ) and accuracy (0.83-0.98) were observed across all diagnoses
<b>Shoulder</b>					
Dratsch (2023)	3-T Ingenia (Philips Healthcare)	2D CS vs. CS-AI (2,3, 4, 6 and 8) 3D CS vs. CS-AI (8, 10, and 13)	2D TSE PDWI 3D TSE PDWI	2D CS-AI 4 (40%), CS-AI 6 (53%), CS-AI 8 (62%), 3D CS-AI 10 (19%), CS-AI 13 (38%)	Both 2D and 3D sequences reconstructed using CS-AI demonstrated significantly superior subjective and objective image quality compared to sequences reconstructed using CS with similar acceleration factors. 2D sequences achieved a 4-fold acceleration and 3D sequences achieved 13-fold acceleration
Liu (2024)	3-T SIGNATM Premier (GE Healthcare)	Standard vs. CS-AI	2D TSE PDWI-FS, T1WI	54.70%	CS-AI significantly reduced scan time by approximately 54.7%, while simultaneously enhancing image quality compared to standard sequences. Moreover, CS-AI proved to be particularly valuable in detecting subacromial and subcoracoid bursa thickening
<b>Ankle</b>					
Foreman (2022)	3-T Ingenia Elition (Philips Healthcare)	CS (2.5) vs. CS-AI (5.1-7.6) vs. high resolution CS-AI (CSAHR)	2D TSE T2WI, T1WI	CS-AIx2 (47%), CS-AIx3 (63%)	There were no notable differences in structural depiction between CS and CS-AIx2, as both protocols identified the same abnormalities. However, CS-AIx3 showed a slightly lower depiction, though most abnormalities were still detected
Zhao (2023)	3-T uMR880 (United Imaging Healthcare)	PI vs CS vs. CS-A (2.3-3.8)	2D TSE T2WI, T1WI, PDWI-FS	57%-59% (compared to PI) 62%-67% (compared to CS)	CS-AI acceleration reduces the scanning times of 2D sequences by 32%-43% compared to conventional CS and PI, while preserving image quality

ADLR = advanced deep-learning-based post-processing techniques ("Deep Resolve Boost/Sharp"), CDLR = conventional deep-learning-based post-processing techniques ("Deep Resolve Gain/Sharp"), CS = compressed SENSE, CS-AI = AI assisted compressed sense technology, PI = parallel imaging, PI-CS = conventional reconstructions of compressed SENSE, Standard = fully sampled protocol

clinically unacceptable levels (diagnostically usable images: 75.0% at AF 8; 32.5% at AF 11), while CS-AI maintained clinical usability (95% at AF 8; 70% at AF 11).

Sui et al. (29) reported that CS-AI reduced acquisition time by 18.9% while maintaining comparable SNR and contrast-to-noise ratio (CNR) across all sequences, with no significant qualitative differences between the techniques.

Almansour et al. (30) found that although scan time was reduced by approximately 70%, CS-AI images remained clinically acceptable and comparable to conventional MR images. No significant differences were noted in the detection of major abnormalities ( $p > 0.18$ ) or in assessments of spinal structures and artifacts ( $p > 0.06$ ), though CS-AI images exhibited significantly reduced noise ( $p < 0.001$ ).

Schlicht et al. (31) evaluated DLR postprocessing applied to images acquired using a low-field (0.55 T) MRI system. Two types of DLR methods—conventional (CDLR) and advanced (ADLR)—were applied to images obtained via PI techniques. ADLR images demonstrated superior image quality and resolution compared to CDR (p < 0.001). Quantitatively, cerebrospinal fluid-to-spinal cord signal intensity ratios in the TIRM sequence were significantly higher with ADLR (p < 0.001), while contrast between other structures showed no significant differences (p > 0.10).

## KNEE MRI

Chen et al. (32) showed that a DL-based variational network reconstruction technique maintained image quality in turbo spin-echo (TSE) sequences while improving reconstruction speed compared to conventional PI combined with CS, suggesting its viability for routine clinical use.

Herrmann et al. (4) demonstrated that DLR could reduce acquisition time in musculoskeletal MRI by up to 75%. Despite halved scan times, DLR provided lower image noise and improved edge sharpness (33), while maintaining comparable contrast and artifact levels. Structures such as cartilage, tendons, and ligaments were clearly visualized, though small intraosseous structures appeared less conspicuous than on conventional TSE images.

Johnson et al. (34) extended evaluation beyond image quality to diagnostic performance for knee pathologies, including ligament tears, cartilage lesions, meniscal tears, and bone marrow edema. DL-based imaging with an AF of 4 achieved diagnostic performance comparable to conventional GRAPPA-accelerated imaging (AF 2), while reducing scan time from 9 minutes 56 seconds to 5 minutes 33 seconds and producing higher-quality images.

Iuga et al. (35) applied a hybrid DL-based algorithm, Adaptive-CS-Net, to 2D accelerated knee MRI, combining CS with DL. Unlike fully data-driven methods, this approach selectively replaced portions of the conventional reconstruction pipeline with DL components, offering greater flexibility. Whereas traditional CS is limited by image degradation at high CS factors, the DL-enhanced method enabled higher acceleration without sacrificing image quality. The study demonstrated that sagittal knee images could be acquired in under 2 minutes with a 64% reduction in acquisition time and no significant quality loss. SNR and CNR were statistically higher in CS-AI reconstructions compared to conventional CS.

Chaudhari et al. (19, 20) developed a DL-based super-resolution technique called DeepResolve, which transforms low-resolution images into high-resolution 3D DESS knee images. Applied to osteoarthritis imaging, DeepResolve improved structural similarity, peak SNR, and

root mean square error. The method enhanced image quality and sharpness without compromising cartilage segmentation accuracy and facilitated osteophyte detection.

Wang et al. (36) proposed a 2-minute AI-assisted compressed sensing protocol for detecting meniscal tears, cruciate ligament injuries, and cartilage defects. This method achieved diagnostic performance comparable to an 8-minute PI protocol. The ACS protocol included sagittal T1-weighted and three-plane PD-weighted sequences, demonstrating potential for use in patients with severe pain, pediatric populations with limited cooperation, or for trauma screening.

Dratsch et al. (37) applied CS combined with DL to 3D knee MRI in a study of 20 volunteers and evaluated four acceleration levels. Even at a  $10\times$  acceleration, image quality was nearly equivalent to that of conventional  $2\times$  CS images. However, the study's generalizability was limited by its small sample size of healthy participants.

Ni et al. (38) also demonstrated that DL-based 3D CS imaging could replace both conventional 3D CS and 2D PI sequences. The method enabled effective multiplanar reconstruction at 2 mm and 3.5 mm slice thicknesses from 3D data.

## SHOULDER MRI

Dratsch et al. (39) compared 3D and 2D sequences and found that CS-AI provided higher SNRs for muscle and bone and higher CNRs for bone and tendon relative to muscle. Notably, in 3D CS-AI sequences, imaging time was reduced by 38%, yet the subscapularis tendon, bone, and acromioclavicular joint structures were depicted more clearly than with conventional CS imaging. However, no significant differences were observed in 2D sequences.

Liu et al. (40) evaluated image quality and bursal thickness in patients with chronic shoulder pain, comparing conventional MRI with DL-based MRI (DL-MRI). DL-MRI demonstrated superior image quality and fewer artifacts. Additionally, bursal thickness was greater on DL-MRI, and subacromial bursal thickening was more frequently detected on coronal images. The relative SNR (rSNR) of muscles was higher in DL-MRI, while the rSNR of bone on PD-weighted sequences was lower compared to conventional MRI.

## ANKLE MRI

Foreman et al. (41) compared conventional CS and DL-based CS (CS-AI), reporting a 47%–63% reduction in acquisition time depending on the AF. In the highly accelerated  $3\times$  CS-AI protocol, SNRs for fluid and muscle were significantly higher than those in CS ( $p = 0.011$  and  $p = 0.035$ , respectively), and CNRs were higher for all tissue types ( $p = 0.011$ ).

When evaluating ankle ligaments using conventional CS images as a reference, the  $2\times$  CS-AI images showed no significant difference, while the  $3\times$  CS-AI images received lower qualitative scores ( $p < 0.001$ ). High-resolution CS-AI images provided better visualization of structures such as the peroneal tendons, tibial bone, anterior talofibular ligament, and extensor tendons. Most pathologies identified in CS were also detected in the  $2\times$  and  $3\times$  CS-AI images, except for a peroneus brevis tendon split tear and bone marrow edema smaller than 3 mm in the  $3\times$  CS-AI images. However, diagnostic confidence was slightly lower for abnormalities detected in the  $3\times$  CS-AI images.

Zhao et al. (42) compared PI, CS, and CS-AI and found that CS-AI with an AF of 3.3 yielded the best overall performance. The CS-AI protocol reduced acquisition times by 57%–59% com-

pared to PI and 62%–67% compared to CS. Quantitative analysis showed that CS-AI had higher SNRs than PI in most anatomical structures except ligaments and tendons, and higher SNRs than CS in all structures except tendons. Similarly, CS-AI demonstrated generally superior CNRs compared to both techniques. While image quality ratings were comparable overall, CS-PI showed higher scores for specific ligaments. All three techniques provided consistent results regarding diagnostic performance for ligament injuries and osteochondral lesions.

## LIMITATIONS OF DLR

### ARTIFACTS DUE TO NOISE REDUCTION IN DLR

DLR is highly effective in reducing Gaussian noise, which is commonly observed in medical imaging. However, since various other artifacts exist in MRI, non-Gaussian artifacts may become more prominent after Gaussian noise is removed (13, 43). A representative example is over-smoothing, in which actual fine structures or lesions may be removed along with noise, resulting in smoother images but with a loss of critical anatomical detail. Another issue is hallucination artifacts, where the network generates structures that do not exist, based on statistical patterns learned from training data. Blurring of details, especially in regions with repetitive structures, is also a known limitation. These artifacts often result from limited diversity in training data, suboptimal loss functions, or excessive regularization. Current research is focused on mitigating such artifacts using techniques such as data diversification, perceptual loss functions, and uncertainty estimation.

### LIMITATIONS IN HANDLING INHOMOGENEOUS NOISE

Training datasets for DL algorithms typically consist of images with homogeneously distributed noise. As a result, networks trained on such data perform well in removing homogeneous noise but show limited effectiveness against inhomogeneous noise. For example, in PI, noise associated with the geometry factor (g-factor) varies depending on coil position and configuration and is unevenly distributed, unlike Gaussian noise. This type of noise often appears as striping patterns, especially in the central regions of the image, making it more difficult to suppress using DLR techniques (44). Since g-factor-related noise is spatially dependent, a more effective strategy involves using a threshold adjusted based on the g-factor map to reduce this inhomogeneous noise.

### INSTABILITY OF DLR

DLR can enhance diagnostic performance by improving the SNR. However, instability in output images has been observed, particularly when small anatomical structures are not accurately reconstructed due to algorithmic limitations (45). Most current DLR research has focused on enhancing image quality, with relatively few studies evaluating its effectiveness in detecting small anatomical abnormalities. Until further validation is available, DLR images should be interpreted alongside conventional reference images obtained via PI techniques. Nevertheless, given the rapid advancement of DLR technology, these limitations are expected to be addressed, and DLR may soon become a standard acquisition method.

## QUANTITATIVE ANALYSIS

It remains unclear whether DLR-processed MR images can yield quantitative outcomes equivalent to those from conventional MR images. Kim et al. (46) reported that radiomic features extracted from CT images may vary depending on the reconstruction method. Similarly, DLR may alter radiomic features in MR imaging, which should be considered when performing quantitative analyses.

## CONCLUSION

Studies across various joint regions—including the spine, knee, shoulder, and ankle—have demonstrated the clinical utility of DL-based MRI reconstruction techniques in accelerating image acquisition and improving image quality by reducing noise and artifacts. Integrating DLR with conventional acceleration techniques, such as PI and CS, has further enhanced these benefits.

Future large-scale studies are necessary to demonstrate the full clinical utility of these techniques not only in image quality improvement but also in disease diagnosis. Additionally, there is increasing demand for the development of advanced technologies such as super-resolution imaging, artifact-corrected imaging, and synthetic MRI. Radiologists should understand the clinical value of DLR techniques and collaborate with MR physicists and engineers to select and implement these technologies effectively in clinical practice.

### Supplementary Materials

Korean translation of this article is available with the Online-only Data Supplement at <https://doi.org/10.3348/jksr.2025.0015>.

### Conflicts of Interest

The author has no potential conflicts of interest to disclose.

### ORCID iD

Hye Jin Yoo  <https://orcid.org/0000-0002-9704-7870>

### Funding

None

## REFERENCES

1. Hamilton J, Franson D, Seiberlich N. Recent advances in parallel imaging for MRI. *Prog Nucl Magn Reson Spectrosc* 2017;101:71-95
2. Priyanka, Kadavigere R, Nayak S S, Chandran M O, Shirlal A, Pires T, et al. Impact of artificial intelligence assisted compressed sensing technique on scan time and image quality in musculoskeletal MRI - a systematic review. *Radiography (Lond)* 2024;30:1704-1712
3. Wang S, Su Z, Ying L, Peng X, Zhu S, Liang F, et al. Accelerating magnetic resonance imaging via deep learning. *Proc IEEE Int Symp Biomed Imaging* 2016;2016:514-517
4. Herrmann J, Koerzdoerfer G, Nickel D, Mostapha M, Nadar M, Gassenmaier S, et al. Feasibility and implementation of a deep learning MR reconstruction for TSE sequences in musculoskeletal imaging. *Diagnostics (Basel)* 2021;11:1484
5. Lin DJ, Johnson PM, Knoll F, Lui YW. Artificial intelligence for MR image reconstruction: an overview for clinicians. *J Magn Reson Imaging* 2021;53:1015-1028

6. Yoon MA, Gold GE, Chaudhari AS. Accelerated musculoskeletal magnetic resonance imaging. *J Magn Reson Imaging* 2024;60:1806-1822
7. Deshmane A, Gulani V, Griswold MA, Seiberlich N. Parallel MR imaging. *J Magn Reson Imaging* 2012;36:55-72
8. Ye JC. Compressed sensing MRI: a review from signal processing perspective. *BMC Biomed Eng* 2019;1:8
9. Geethanath S, Reddy R, Konar AS, Imam S, Sundaresan R, D RR B, et al. Compressed sensing MRI: a review. *Crit Rev Biomed Eng* 2013;41:183-204
10. Wang S, Xiao T, Liu Q, Zheng H. Deep learning for fast MR imaging: a review for learning reconstruction from incomplete k-space data. *Biomed Signal Process Control* 2021;68:102579
11. Baek SD, Lee J, Kim S, Song HT, Lee YH. Artificial intelligence and deep learning in musculoskeletal magnetic resonance imaging. *Investig Magn Reson Imaging* 2023;27:67-74
12. Jeong G, Kim H, Yang J, Jang K, Kim J. All-in-one deep learning framework for MR image reconstruction. arXiv [Preprint]. 2024. Available at: <https://doi.org/10.48550/arXiv.2405.03684>. Accessed February 1, 2025
13. Kiryu S, Akai H, Yasaka K, Tajima T, Kunimatsu A, Yoshioka N, et al. Clinical impact of deep learning reconstruction in MRI. *Radiographics* 2023;43:e220133
14. Montalt-Tordera J, Muthurangu V, Hauptmann A, Steeden JA. Machine learning in magnetic resonance imaging: image reconstruction. *Phys Med* 2021;83:79-87
15. Chen YT, Schonlieb CB, Lio P, Leiner T, Dragotti PL, Wang G, et al. AI-based reconstruction for fast MRI—a systematic review and meta-analysis. *Proc IEEE* 2022;110:224-245
16. Huang J, Fang Y, Nan Y, Wu H, Wu Y, Gao Z, et al. Data and physics driven learning models for fast MRI - fundamentals and methodologies from CNN, GAN to attention and transformers. arXiv [Preprint]. 2019. Available at: <https://doi.org/10.48550/arXiv.2204.01706>. Accessed February 1, 2025
17. Liang D, Cheng J, Ke Z, Ying L. Deep MRI reconstruction: unrolled optimization algorithms meet neural networks. arXiv [Preprint]. 2019. Available at: <https://doi.org/10.48550/arXiv.1907.11711>. Accessed February 1, 2025
18. Zeng K, Zheng H, Cai C, Yang Y, Zhang K, Chen Z. Simultaneous single- and multi-contrast super-resolution for brain MRI images based on a convolutional neural network. *Comput Biol Med* 2018;99:133-141
19. Chaudhari AS, Fang Z, Kogan F, Wood J, Stevens KJ, Gibbons EK, et al. Super-resolution musculoskeletal MRI using deep learning. *Magn Reson Med* 2018;80:2139-2154
20. Chaudhari AS, Stevens KJ, Wood JP, Chakraborty AK, Gibbons EK, Fang Z, et al. Utility of deep learning super-resolution in the context of osteoarthritis MRI biomarkers. *J Magn Reson Imaging* 2020;51:768-779
21. Neubert A, Bourgeat P, Wood J, Engstrom C, Chandra SS, Crozier S, et al. Simultaneous super-resolution and contrast synthesis of routine clinical magnetic resonance images of the knee for improving automatic segmentation of joint cartilage: data from the osteoarthritis initiative. *Med Phys* 2020;47:4939-4948
22. Qiu D, Zhang S, Liu Y, Zhu J, Zheng L. Super-resolution reconstruction of knee magnetic resonance imaging based on deep learning. *Comput Methods Programs Biomed* 2020;187:105059
23. Chaudhari A, Fang Z, Lee JH, Gold G, Hargreaves B. Deep learning super-resolution enables rapid simultaneous morphological and quantitative magnetic resonance imaging. In Knoll F, Maier A, Rueckert D, eds. *Machine learning for medical image reconstruction*. Cham: Springer 2018:3-11
24. Sommer K, Saalbach A, Brosch T, Hall C, Cross NM, Andre JB. Correction of motion artifacts using a multi-scale fully convolutional neural network. *AJNR Am J Neuroradiol* 2020;41:416-423
25. Küstner T, Armanious K, Yang J, Yang B, Schick F, Gatidis S. Retrospective correction of motion-affected MR images using deep learning frameworks. *Magn Reson Med* 2019;82:1527-1540
26. Desai AD, Gunel B, Ozturkler BM, Beg H, Vasanawala S, Hargreaves BA, et al. VORTEX: physics-driven data augmentations using consistency training for robust accelerated MRI reconstruction. Available at: <https://proceedings.mlr.press/v172/desai22a.html>. Published 2022. Accessed February 1, 2025
27. Singh NM, Dey N, Hoffmann M, Fischl B, Adalsteinsson E, Frost R, et al. Data consistent deep rigid MRI motion correction. *Proc Mach Learn Res* 2024;227:368-381
28. Fervers P, Zaeske C, Rauen P, Iuga AI, Kottlors J, Persigehl T, et al. Conventional and deep-learning-based image reconstructions of undersampled k-space data of the lumbar spine using compressed sensing in MRI: a comparative study on 20 subjects. *Diagnostics (Basel)* 2023;13:418
29. Sui H, Gong Y, Liu L, Lv Z, Zhang Y, Dai Y, et al. Comparison of artificial intelligence-assisted compressed sensing (ACS) and routine two-dimensional sequences on lumbar spine imaging. *J Pain Res* 2023;16:257-267
30. Almansour H, Herrmann J, Gassenmaier S, Afat S, Jacoby J, Koerzdoerfer G, et al. Deep learning recon-

struction for accelerated spine MRI: prospective analysis of interchangeability. *Radiology* 2023;306:e212922

31. Schlicht F, Vosshenrich J, Donners R, Seifert AC, Fenchel M, Nickel D, et al. Advanced deep learning-based image reconstruction in lumbar spine MRI at 0.55 T - effects on image quality and acquisition time in comparison to conventional deep learning-based reconstruction. *Eur J Radiol Open* 2024;12:100567
32. Chen F, Taviani V, Malkiel I, Cheng JY, Tamir JL, Shaikh J, et al. Variable-density single-shot fast spin-echo MRI with deep learning reconstruction by using variational networks. *Radiology* 2018;289:366-373
33. Kim M, Lee SM, Park C, Lee D, Kim KS, Jeong HS, et al. Deep learning-enhanced parallel imaging and simultaneous multislice acceleration reconstruction in knee MRI. *Invest Radiol* 2022;57:826-833
34. Johnson PM, Lin DJ, Zbontar J, Zitnick CL, Sriram A, Muckley M, et al. Deep learning reconstruction enables prospectively accelerated clinical knee MRI. *Radiology* 2023;307:e220425
35. Iuga AI, Rauen PS, Siedek F, Große-Hokamp N, Sonnabend K, Maintz D, et al. A deep learning-based reconstruction approach for accelerated magnetic resonance image of the knee with compressed sense: evaluation in healthy volunteers. *Br J Radiol* 2023;96:20220074
36. Wang Q, Zhao W, Xing X, Wang Y, Xin P, Chen Y, et al. Feasibility of AI-assisted compressed sensing protocols in knee MR imaging: a prospective multi-reader study. *Eur Radiol* 2023;33:8585-8596
37. Dratsch T, Zäske C, Siedek F, Rauen P, Hokamp NG, Sonnabend K, et al. Reconstruction of 3D knee MRI using deep learning and compressed sensing: a validation study on healthy volunteers. *Eur Radiol Exp* 2024;8:47
38. Ni M, He M, Yang Y, Wen X, Zhao Y, Gao L, et al. Application research of AI-assisted compressed sensing technology in MRI scanning of the knee joint: 3D-MRI perspective. *Eur Radiol* 2024;34:3046-3058
39. Dratsch T, Siedek F, Zäske C, Sonnabend K, Rauen P, Terzis R, et al. Reconstruction of shoulder MRI using deep learning and compressed sensing: a validation study on healthy volunteers. *Eur Radiol Exp* 2023;7:66
40. Liu Z, Wen B, Wang Z, Wang K, Xie L, Kang Y, et al. Deep learning-based reconstruction enhances image quality and improves diagnosis in magnetic resonance imaging of the shoulder joint. *Quant Imaging Med Surg* 2024;14:2840-2856
41. Foreman SC, Neumann J, Han J, Harrasser N, Weiss K, Peeters JM, et al. Deep learning-based acceleration of compressed sense MR imaging of the ankle. *Eur Radiol* 2022;32:8376-8385
42. Zhao Q, Xu J, Yang YX, Yu D, Zhao Y, Wang Q, et al. AI-assisted accelerated MRI of the ankle: clinical practice assessment. *Eur Radiol Exp* 2023;7:62
43. Zaitsev M, McLaren J, Herbst M. Motion artifacts in MRI: a complex problem with many partial solutions. *J Magn Reson Imaging* 2015;42:887-901
44. Robson PM, Grant AK, Madhuranthakam AJ, Lattanzi R, Sodickson DK, McKenzie CA. Comprehensive quantification of signal-to-noise ratio and g-factor for image-based and k-space-based parallel imaging reconstructions. *Magn Reson Med* 2008;60:895-907
45. Antun V, Renna F, Poon C, Adcock B, Hansen AC. On instabilities of deep learning in image reconstruction and the potential costs of AI. *Proc Natl Acad Sci U S A* 2020;117:30088-30095
46. Kim H, Park CM, Lee M, Park SJ, Song YS, Lee JH, et al. Impact of reconstruction algorithms on CT radiomic features of pulmonary tumors: analysis of intra- and inter-reader variability and inter-reconstruction algorithm variability. *PLoS One* 2016;11:e0164924

## 근골격 자기공명영상에서의 딥러닝 기반 영상 재구성 기법

류혜진\*

자기공명영상(이하 MRI)은 근골격계의 복잡한 해부학적 구조를 평가하기 위한 고화질 영상을 얻는 데 필수적이다. 하지만 긴 촬영 시간으로 인해 환자의 불편함을 증가시킬 수 있고 움직으로 인한 인공물이 발생하면서 오히려 영상 질이 저하될 수 있다. 이러한 문제점을 해결하기 위해 짧은 시간 내에 고품질 영상을 얻기 위한 Sensitivity Encoding (SENSE)와 Generalized Autocalibrating Partial Parallel Acquisition (GRAPPA)와 같은 가속화 영상 촬영 기법이 개발되었다. 이후 iteration을 활용하여 부족한 k-공간 데이터를 재구성하는 compressed sensing 기법이 등장하였다. 최근에는 딥러닝 기반 영상 재구성 기술이 등장하여, 더 우수한 신호 대 잡음비와 높은 가속 인자를 제공하고 있다. 척추, 무릎, 발목, 어깨 등 다양한 관절에서 딥러닝 기반 영상 재구성 기술은 촬영 시간을 크게 단축시키면서도 기존 영상과 비슷한 정도의 영상 질과 진단능을 보이고 있어 임상적 활용이 넓어지고 있다. 또한, 낮은 자장 MRI 영상 해상도를 향상시키고, 여러 가지 인공물을 교정하는 등의 다양한 연구도 진행 중이며, 이러한 첨단 기술들의 활용 가능성은 더욱 확대되고 있다.

서울대학교병원 영상의학과